Retinal guanylyl cyclase activation by calcium sensor proteins mediates photoreceptor degeneration in an *rd3* mouse model of congenital human blindness

Received for publication, June 25, 2019, and in revised form, July 22, 2019 Published, Papers in Press, July 25, 2019, DOI 10.1074/jbc.RA119.009948

Alexander M. Dizhoor[1], **Elena V. Olshevskaya, and Igor V. Peshenko**

From the Pennsylvania College of Optometry, Salus University, Elkins Park, Pennsylvania 19027

Edited by Roger J. Colbran

Deficiency of RD3 (retinal degeneration 3) protein causes recessive blindness and photoreceptor degeneration in humans and in the *rd3* mouse strain, but the disease mechanism is unclear. Here, we present evidence that RD3 protects photoreceptors from degeneration by competing with guanylyl cyclase-activating proteins (GCAPs), which are calcium sensor proteins for retinal membrane guanylyl cyclase (RetGC). RetGC activity in *rd3*/*rd3* retinas was drastically reduced but stimulated by the endogenous GCAPs at low Ca^{2+} concentrations. RetGC activity completely failed to accelerate in *rd3*/*rd3GCAPs*$^{-/-}$ hybrid photoreceptors, whose photoresponses remained drastically suppressed compared with the WT. However, ~70% of the hybrid *rd3*/*rd3GCAPs*$^{-/-}$ photoreceptors survived past 6 months, in stark contrast to <5% in the nonhybrid *rd3*/*rd3* retinas. GFP-tagged human RD3 inhibited GCAP-dependent activation of RetGC *in vitro* similarly to the untagged RD3. When transgenically expressed in *rd3*/*rd3* mouse retinas under control of the rhodopsin promoter, the RD3GFP construct increased RetGC levels to near normal levels, restored dark-adapted photoresponses, and rescued rods from degeneration. The fluorescence of RD3GFP in *rd3*/*rd3RD3GFP*$^{+}$ retinas was mostly restricted to the rod photoreceptor inner segments, whereas GCAP1 immunofluorescence was concentrated predominantly in the outer segment. However, RD3GFP became distributed to the outer segments when bred into a *GCAPs*$^{-/-}$ genetic background. These results support the hypothesis that an essential biological function of RD3 is competition with GCAPs that inhibits premature cyclase activation in the inner segment. Our findings also indicate that the fast rate of degeneration in RD3-deficient photoreceptors results from the lack of this inhibition.

Production of cGMP in photoreceptors by retinal membrane RetGC[2] (isozymes RetGC1, *GUCY2D*) and RetGC2 (*GUCY2F*) (1–3) imparts light sensitivity to vertebrate photoreceptors by maintaining inward cation current via cGMP-gated channels in their outer segments. When light-activated phosphodiesterase hydrolyzes cGMP, rods and cones hyperpolarize by closing the cGMP-gated channels (reviewed in Refs. 4–6). RetGC becomes accelerated after illumination, which allows photoreceptors to recover and adapt to light and then decelerate as photoreceptors recover from the excitation (reviewed in Refs. 7 and 8). Two types of regulatory proteins control RetGC activity in photoreceptors. Calcium sensor proteins (GCAPs) (1, 9–11) stimulate the cyclase in the light and decelerate it in the dark, following the respective decline and rise of free calcium concentrations (12–16). RD3 (retinal degeneration 3) protein (17, 18) enhances RetGC content in photoreceptor outer segment membranes, possibly by promoting the delivery of the enzyme to the outer segment (19, 20). At the same time, RD3 strongly inhibits the cyclase *in vitro*, by suppressing both the basal and the GCAP-stimulated activities of RetGC1 and RetGC2 (21, 22). Truncations of RD3 have been linked to a severe recessive blindness, Leber's congenital amaurosis 12 (LCA12), in human patients (17, 23). A similar recessive nonsense mutation causes rapid degeneration of photoreceptors in *rd3* mouse strain (17, 22). The lack of RD3 strongly lowers RetGC1 and RetGC2 content in their photoreceptors (19, 20, 22). However, *rd3* photoreceptors degenerate faster and more severely than photoreceptors completely devoid of both ReGC1 and RetGC2 (22), thus suggesting that the inhibitory activity of RD3, along with the maintaining proper RetGC content, is essential for the survival of photoreceptors. Here, we present evidence in support of this hypothesis. Our results indicate that prevention of RetGC activation by GCAPs in the inner segment is a critical biological function of RD3 in photoreceptor physiology.

Results

Guanylyl cyclase activity and retinal histology in rd3/rd3GCAPs$^{-/-}$ *versus rd3/rd3 mice*

Consistent with the original observation by Azadi *et al.* (19), the lack of RD3 caused a strong reduction in RetGC expression (Fig. 1*A*) and activity (Fig. 1*B*) in homozygous *rd3*/*rd3* retinas. The RetGC activity in *rd3*/*rd3* retinas aged 3.5 weeks (mean ± S.D., *n*) in the presence of Ca^{2+} was strongly suppressed (0.0091 ± 0.0024 nmol cGMP/min/retina, 5, *versus* 0.04 ± 0.007, 7, in WT; $p < 0.0001$, ANOVA/Bonferroni post hoc).

This work was supported by National Institutes of Health Grant EY011522 and by the Pennsylvania Department of Health. The authors declare that they have no conflicts of interest with the contents of this article. The content is solely the responsibility of the authors and does not necessarily represent the official views of the National Institutes of Health.

[1] To whom correspondence should be addressed: Research S416, Salus University, 8360 Old York Rd., Elkins Park, PA 19027. Tel.: 215-780-1468; Fax 215-780-1464; E-mail: adizhoor@salus.edu.

[2] The abbreviations used are: RetGC, retinal membrane guanylyl cyclase; DIC, differential image contrast; ERG, electroretinography; GAPDH, glyceraldehyde-3-phosphate dehydrogenase; GCAP, guanylyl cyclase-activating protein; ANOVA, analysis of variance; CI, confidence interval.

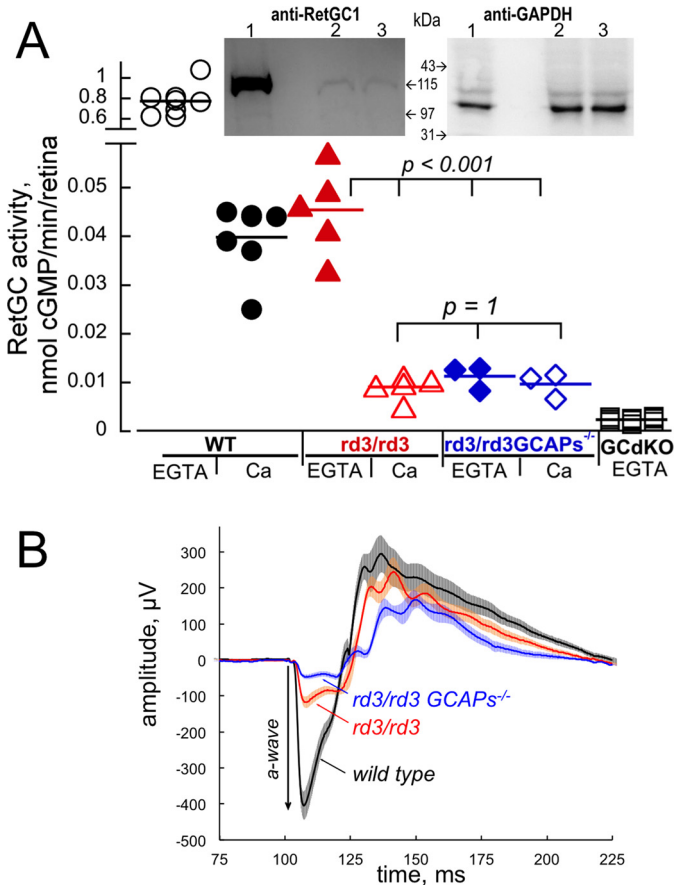

Figure 1. Deletion of GCAPs further disables RetGC activity in *rd3/rd3* photoreceptors. *A*, RetGC activity in the dark-adapted retinas from 3.5-week-old WT (*black open circles* and *black filled circles*), *rd3/rd3* (*red filled triangles* and *red open triangles*), and *rd3/rd3GCAPs*$^{-/-}$ (*blue filled diamonds* and *blue open diamonds*) measured in the presence of EGTA (*black open circles*, *red filled triangles*, and *blue filled diamonds*) or 10 μM Ca^{2+} (*black filled circles*, *red open triangles*, and *blue open diamonds*). Nonphotoreceptor guanylyl cyclase activity background in the presence of EGTA (□) was measured in RetGC1$^{-/-}$ RetGC2$^{-/-}$ double knockouts retinas. Note the *y*-axis scale change after the break. The differences were tested by ANOVA ($F = 104$; $p < 0.0001$) and Bonferroni post hoc pairs comparison (99% CI, $\alpha = 0.01$). The *p* values shown in the graph are from the post hoc test. *Inset*, RetGC1 Western immunoblots (equivalent of ~0.2 retina/lane in each case): WT (*lane 1*), *rd3/rd3* (*lane 2*), and *rd3/rd3GCAPs*$^{-/-}$ (*lane 3*). The blots were probed with anti-RetGC1 (*left*) or anti-GAPDH antibodies (*right*). *B*, dark-adapted (scotopic) ERG recorded in WT (*black trace*), *rd3/rd3* (*red trace*), and *rd3/rd3GCAPs*$^{-/-}$ (*blue trace*) at 1 month of age in response to a saturating 1-ms 505-nm flash of 1×10^6 photons/rod, delivered at 100 ms. The traces are averaged (mean ± S.E., *error bars*) from 12, 10, and 9 mice of the respective genotypes. The differences of the a-wave amplitudes (ANOVA, $F = 41$; $p < 0.0001$) when compared with the WT (404 ± 40 μV) using Bonferroni post hoc test were significant ($p < 0.0001$) both in *rd3/rd3* (117 ± 16 μV) and in *rd3/rd3GCAPs*$^{-/-}$ (47 ± 7 μV).

However, despite being heavily reduced as compared with the maximal activity in WT (0.8 ± 0.2 nmol cGMP/min/retina, 8; $p < 0.0001$), the cyclase activity remaining in *rd3/rd3* retinas remained stimulated at least 5-fold by the endogenous GCAPs in the presence of EGTA (0.045 ± 0.01 nmol cGMP/min/retina, 5, $p < 0.0001$; Fig. 1*A*).

We reasoned that if the *rd3/rd3* photoreceptors rapidly degenerate because of the low cyclase activity, then a complete removal of GCAPs would additionally suppress activation of the remaining cyclase, further lower cGMP production and thus exacerbate degeneration. Conversely, if the *rd3/rd3* photoreceptor degeneration mainly resulted from aberrant, nonrestricted by RD3, activation of the cyclase by GCAPs, then deletion of GCAPs could protect *rd3/rd3* photoreceptors. Indeed, deletion of GCAPs further reduced cGMP production in *rd3/rd3GCAPs*$^{-/-}$ hybrids. Their RetGC content did not increase (Fig. 1*A*, *inset*, *lane 3*), and the RetGC activity not only remained much lower than in WT in the presence of Ca^{2+} (0.01 ± 0.003 nmol/min/retina, 3, $p < 0.0001$), but also, in contrast to *rd3rd3*, now failed to accelerate even at low Ca^{2+} concentrations because of the lack of the endogenous GCAPs (0.011 ± 0.003 nmol/min/retina, 3, $p < 0.0001$). Consistent with the deficiency of cGMP production, dark-adapted electroretinography (ERG) response to a saturating bright flash in both *rd3/rd3* mice and the *rd3/rd3GCAPs*$^{-/-}$ hybrids remained drastically suppressed compared with the WT (Fig. 1*B*). At 1 month of age, the amplitude (mean ± S.E., *n*) of the ERG a-wave—the negative corneal voltage deflection produced by closure of cGMP-gated channels in photoreceptors—was strongly reduced compared with the WT ($p < 0.0001$), from 404 ± 40 μV, 12, in WT to 117 ± 16 μV, 10, in *rd3/rd3* and 47 ± 7 μV, 9, in *rd3/rd3GCAPs*$^{-/-}$.

Nonetheless, despite further reduction in their RetGC activity, degeneration of photoreceptors in *rd3/rd3GCAPs*$^{-/-}$ hybrids was dramatically decelerated when compared with *rd3/rd3*. In *rd3/rd3*, photoreceptor nuclei count rapidly declined within several months (Fig. 2, *A* and *B*). After 6 months, only ~3% of nuclei were identifiable in what remained of the photoreceptor layer (marked *yellow*), and the outer segments stratum was completely absent. In contrast, the *rd3/rd3GCAPs*$^{-/-}$ hybrids at that age displayed much lesser (≤30%, $p < 0.0001$) reduction in photoreceptor count and nearly normal stratification of the retina: ~70% of the photoreceptors were still present and retained identifiable photoreceptor outer segments layer (Fig. 2, *C* and *D*). Therefore the evidence argued that RD3 ability to block activation of the cyclase by GCAPs was essential for preventing fast degeneration of photoreceptors, but the cellular compartment where RD3 acted in that capacity remained to be clarified.

RD3GFP substitutes for the endogenous RD3 in rd3/rd3 rods

Localization of RD3 in different studies presented a rather controversial issue (19, 20, 23), evidently because of low content of RD3 and potential nonspecific cross-reactivity of different antibodies. A potential masking of the epitope in the outer segment could also influence immunochemical detection of RD3. Therefore, to establish the RD3 localization, we not only applied immunofluorescence detection as described further in the next section but also used fluorescently tagged RD3 (Fig. 3). For that, we first verified that RD3GFP expressed in *Escherichia coli* could substitute the nontagged WT RD3 *in vitro*. Similarly to the WT RD3 (21, 22), the RD3GFP shifted the dose dependence of RetGC activation by GCAP to higher concentrations range and reduced the catalytic activity of the enzyme (Fig. 3*A*). Like a nontagged RD3, 1 μM RD3GFP completely inhibited activation of the recombinant RetGC1 by GCAP1 with only a minor increase in the EC_{50} (~6 nM *versus* 2 nM) (Fig. 3*B*). We therefore reasoned that RD3GFP should be able to functionally substitute for the endogenous RD3 when expressed in mouse photoreceptors.

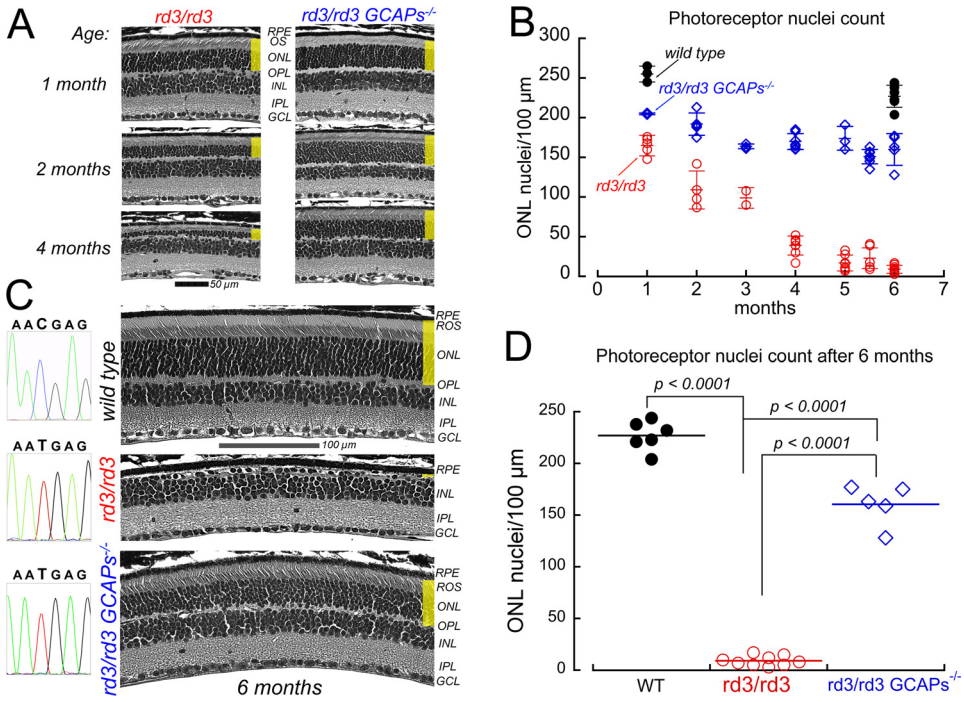

Figure 2. Deletion of GCAPs rescues *rd3/rd3* photoreceptors. *A*, representative retinal morphology at 1, 2 and 4 months of age in *rd3/rd3* (*left panel*) and *rd3/rd3GCAPs*$^{-/-}$ (*right panel*); here and further the markings of retinal histological layers are as follows: *RPE*, retinal pigment epithelium; *ROS*, rod outer segments; *ONL*, outer nuclear layer; *OPL*, outer plexiform layer; *INL*, inner nuclear layer; *IPL*, inner plexiform layer; and *GCL*, ganglion cell layer. The photoreceptor layer thickness between the retinal pigment epithelium and outer plexiform layer is highlighted *yellow*. *B*, changes in photoreceptor nuclei count in the outer nuclear layer with age in WT (*black filled circles*), *rd3/rd3* (*red open circles*), and *rd3/rd3GCAPs*$^{-/-}$ (*blue open diamonds*); *error bars* indicate ± S.D. Each data point was from a different mouse. *C*, representative retinal morphology at 6 months of age in WT (*top panel*), *rd3/rd3* (*middle panel*), and *rd3/rd3GCAPs*$^{-/-}$ (*bottom panel*). The respective sequences from the exon 3 of the *Rd3* mouse gene coding for the WT RD3 and *rd3* mutation are presented on the *left*. Note that *rd3/rd3* and *rd3/rd3GCAPs*$^{-/-}$ mice both carry the homozygous C → T *rd3* substitution. *D*, photoreceptor nuclei count in the outer nuclear layer in 6-month-old WT (*black filled circles*), *rd3/rd3* (*red open circles*), and *rd3/rd3GCAPs*$^{-/-}$ (*blue open diamonds*) mice. Each data point is from a different mouse. The differences were tested by ANOVA ($F = 576$, $p < 0.0001$) and Bonferroni post hoc pairs comparison (99% CI, $\alpha = 0.01$). The *p* values shown in the graph are from the post hoc test.

The transgenic expression of the RD3GFP was guided to mouse retina rods using a 4.2-kb rod opsin promoter (24) (Fig. 3*C*). Following PCR detection of the transgene in the progeny of the RD3GFP-positive founders (Fig. 3*C*, *right panel*), they were subsequently bred into a homozygous *rd3/rd3* background, and the expression of RD3 was verified by Western immunoblotting of the retinal extracts (Fig. 3*D*). In contrast to the WT, the endogenous RD3 was undetectable in *rd3/rd3* and *rd3/rd3RD3GFP*$^{+}$ littermates, but the latter had clearly detectable GFP-tagged RD3. RD3GFP expression strongly, to the levels typical for the WT, elevated the expression of both RetGC1 and RetGC2 in *rd3/rd3RD3GFP*$^{+}$, barely detectable in their non-transgenic *rd3/rd3* littermates.

The RD3GFP expressed in mouse rods fully substituted for the endogenous RD3 in biochemical and physiological tests. RetGC activity in the *rd3/rd3RD3GFP*$^{+}$ retinas became nearly normal. The maximal activity (mean ± S.D., *n*) of the cyclase in the presence of EGTA in *rd3/rd3RD3GFP*$^{+}$ retinas at 1 month of age increased 14-fold when compared with the nontransgenic *rd3/rd3* siblings, to 0.62 ± 0.03 nmol cGMP/min/retina ($p < 0.0001$, ANOVA/Bonferroni post hoc), not significantly lower than the WT (0.77 ± 0.18 nmol cGMP/min/retina; $p = 0.2$) (Fig. 3*E*, *inset*). Ca^{2+} sensitivity of the cyclase regulation in *rd3rd3RD3GFP*$^{+}$ retinas was also similar to the WT retinas (Fig. 3*E*). The RD3GFP rescued rod photoresponse in living animals as well (Fig. 3*F*). The ERG a-wave to saturating flash in dark-adapted WT mice presents mostly rod response with only a small contribution from cones (>97% of all photoreceptors in a mouse retinas are rods) (25). The maximal amplitude (mean ± S.E., *n*) of the dark-adapted ERG a-wave in *rd3/rd3 RD3GFP*$^{+}$ mice at 1 month of age (416 ± 48 μV, 14) became dramatically larger than in *rd3/rd3* siblings (95 ± 9 μV, 24; $p < 0.0001$) and matched the WT (387 ± 40 μV, $n = 9$; $p = 1$). The *rd3/rd3* rods expressing RD3GFP also became resistant to degeneration (Fig. 4). Dark-adapted ERG a-wave (Fig. 4*A*) in *rd3/rd3 RD3GFP*$^{+}$ mice after 4 months of age remained similar to the WT (436 ± 36 μV, 14, and 400 ± 34 μV, 12, respectively; $p = 1$), both drastically different from the rudimentary a-wave of the *rd3/rd3* mice in that age group (20 ± 9 μV, 13; $p < 0.0001$). The preservation of the photoreceptor function, however, was less efficient in cones, consistently with the RD3GFP being expressed under primarily a rod-specific promoter. In light-adapted mice, conditions when rods are saturated and only cone ERG remains detectable, the cone a-wave amplitude (Fig. 4*B*) was rudimentary in *rd3/rd3* (3.8 ± 1 μV) as compared with WT (18.7 ± 1.4 μV; $p < 0.0001$). It slightly improved in *rd3/rd3RD3GFP*$^{+}$ (10.4 ± 1.9 μV) compared with the *rd3rd3* ($p = 0.012$) but remained significantly lower than in WT ($p = 0.0013$). The morphology of the *rd3/rd3RD3GFP*$^{+}$ retinas after 4 months of age showed normal thickness of photoreceptor layer, and in a stark contrast to their *rd3/rd3* littermates, their photoreceptor nuclei count did not significantly differ from the

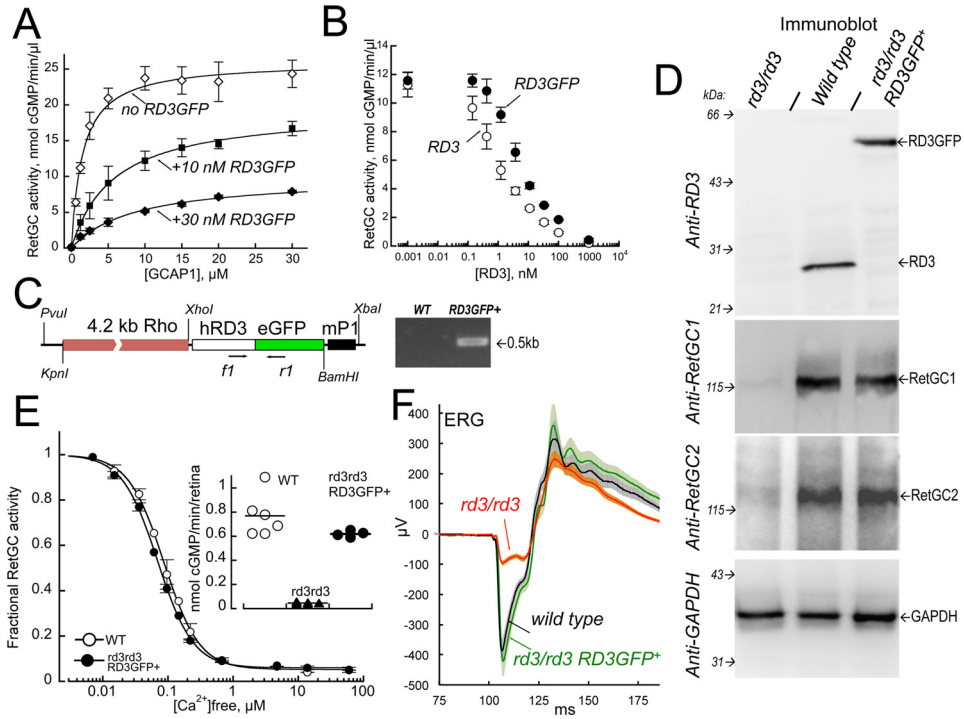

Figure 3. RD3 GFP can substitute for the endogenous RD3 in *rd3/rd3* rods. *A* and *B*, inhibition of the GCAP1-stimulated RetGC1 activity by purified RD3GFP expressed in *E. coli*. *A*, the dose dependence of recombinant RetGC1 activation in HEK293 cells membranes reconstituted with purified GCAP1 in the absence (*open diamonds*) or in the presence of 10 nM (*filled squares*) or 30 nM (*filled diamonds*) purified recombinant RD3GFP; assayed in 2 mM EGTA/10 mM Mg^{2+}. *B*, dose dependence of GCAP-activated RetGC1 inhibition by nontagged WT RD3 (*open circles*) and RD3GFP (*filled circles*). The recombinant RetGC1 was reconstituted with 1 μM purified GCAP1 in the presence of 2 mM EGTA and 10 mM Mg^{2+}. *C*, *left panel*, construct for transgenic expression of RD3GFP in mouse retinas: *Rho*, 4.2-kb rod opsin promoter; *hRD3*, human RD3 cDNA; *eGFP*, enhanced GFP cDNA; *mP1*, mouse protamine 1 gene fragment containing polyadenylation signal; *f1* and *r1*, positions of the forward and the reverse primers used for PCR amplification of the RD3GFP transgene in mouse tail DNA samples. *Right panel*, identification of the *RD3GFP*$^+$ mouse tail DNA using a characteristic 0.5-kb fragment amplified with the f1 and r1 primers. *D*, immunoblotting of proteins extracted from *rd3/rd3*, WT, and *rd3/rd3 RD3GFP*$^+$ retinas (equivalent of ~0.2 retina/lane). The blots were probed with (*top panel* to *bottom panel*): anti-RD3, anti-RetGC1, anti-RetGC2 or anti-GAPDH antibodies. *E*, calcium sensitivity of RetGC in the WT (*open circles*) and *rd3/rd3 RD3GFP*$^+$ (*filled circles*) retina homogenates. The fractional rate of cGMP production in each case was normalized per maximal activity in the absence of Ca^{2+}. *Inset*, the maximal activities of RetGC (nmol cGMP/min/retina) in WT (*open circles*), *rd3/rd3* (*filled triangles*), and *rd3/rd3 RD3GFP*$^+$ (*filled circles*) retinas; the differences in activities (ANOVA, $F = 58$; $p < 0.0001$) when compared using Bonferroni post hoc test were significant between *rd3/rd3* (0.046 ± 0.01 nmol cGMP/min/retina) and both *rd3/rd3RD3GFP*$^+$ (0.62 ± 0.03 nmol cGMP/min/retina) and WT (0.77 ± 0.18 nmol cGMP/min/retina) ($p < 0.0001$), but not between *rd3/rd3RD3GFP*$^+$ and the WT ($p = 0.2$). The cyclase activity was assayed in the dark-adapted retinas under IR illumination as described under "Experimental procedures." *F*, dark adapted ERG (1-ms 505-nm flash of 1×10^6 photons/rod) at 1 month of age in wild type (*black trace*), *rd3/rd3* (*red trace*), and *rd3/rd3RD3GFP*$^+$ (*green trace*).

WT (Fig. 4, *C* and *D*). No evidence of retinal degeneration was seen in three *rd3/rd3 RD3GFP*$^+$ mice even past 6 months (not shown).

RD3 localization in the retina

Polyclonal antibody raised against purified recombinant mouse RD3 indicated that RD3 was present in the inner rather than the outer segment of photoreceptors (Fig. 5*A*). The immunofluorescence in the photoreceptor layer probed with the anti-RD3 antibody was evident in the inner segments and cell bodies but virtually undetectable in the outer segments. The antibody also nonspecifically cross-reacted with inner retina neurons, both in WT and in *rd3/rd3* (not shown), but the signal in photoreceptors was not observed in homozygous *rd3/rd3* mice, arguing for its specificity in photoreceptors (Fig. 5*A*, *lower panel*).

The RD3GFP fluorescence of the transgenically expressed product was present only in photoreceptors and most brightly between the external limiting membrane and the outer segment layer. RD3GFP fluorescence (Fig. 5, *B–E*) was predominantly localized to the rod inner segment, cell bodies, and synaptic terminals (Fig. 5*B*), but very little of the RD3 fluorescence was detectable in rod outer segments (Fig. 5, *C* and *D*). It was clearly separated from both peripherin (Fig. 5*D*) and GCAP1 (Fig. 5*E*) immunofluorescence accumulated in the outer segments.

Expression of the RD3GFP transgene in cones, if any at all, was much lower than in rods (Fig. 5, *F* and *G*). Cones, identified using counterstaining with peanut agglutinin, appeared as dark silhouettes surrounded by the fluorescing rods (Fig. 5*F*). Even though some fluorescence seemingly appeared in the narrow posterior part of sporadic cones after stronger γ correction of the image (Fig. 5*G*), it could be a result of the much brighter fluorescence emission bleeding from the surrounding rods. Moreover, even after the stronger γ-adjustment of the fluorescence images, RD3GFP was observed in the adjacent rod cell bodies but never inside the boundaries of cone cell bodies marked by rhodamine-peanut agglutinin (Fig. 5*G*). Hence, although we cannot exclude that a low-level "leaky" transgene expression in *rd3/rd3RD3GFP*$^+$ cones could occur, the better preservation of cone function (Fig. 4*D*) was more likely due to better protection of cones by averting massive obliteration of the dominating the outer neuronal layer of the retina rods (25). Notably, after deletion of GCAPs by breeding the RD3GFP-

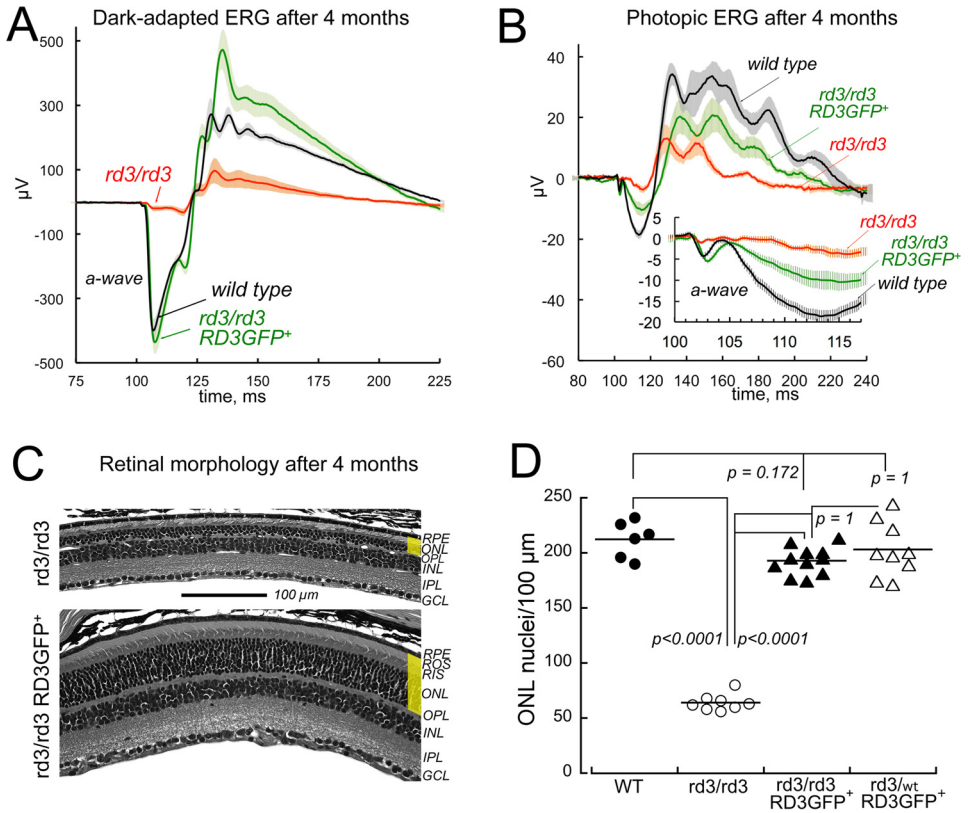

Figure 4. RD3GFP rescues *rd3/rd3* rod degeneration. *A*, dark-adapted (scotopic) ERG recorded in WT (*black trace*), *rd3/rd3* (*red trace*), and *rd3/rd3RD3GFP*$^{+}$ (*green trace*) between 4 and 5 months of age (1-ms 505-nm flash of 1×10^6 photons/rod delivered at 100 ms). The traces are averaged (mean ± S.E., *error bars*) from 14, 13, and 12 mice of each respective genotype; the difference in the a-wave amplitudes (ANOVA, $F = 64$; $p < 0.0001$) was significant between the *rd3/rd3RD3GFP*$^{+}$ (436 ± 36 μV) and *rd3/rd3* (20 ± 9 μV) when compared using Bonferroni post hoc test ($p < 0.0001$), but not between the *rd3/rd3RD3GFP*$^{+}$ and WT (400 ± 36 μV, $p = 1$). *B*, photopic (33×10^3 photons/s/rod, 505-nm light-adapted) M-cone ERG recorded in 11 WT, 11 *rd3/rd3*, and 11 *rd3/rd3 RD3GFP*$^{+}$ mice in response to a 1-ms 505-nm flash, 5.4×10^5 photons/rod; the respective averaged a-wave amplitudes shown in the *inset* on expanded scale are 18.7 ± 1.4 μV; 3.8 ± 1 μV ($p < 0.0001$); and 10.4 ± 1.9 μV ($p = 0.0013$). The differences were evaluated by ANOVA ($F = 25$; $p < 0.0001$) and Bonferroni post hoc pairs comparison (99% CI, $\alpha = 0.01$). The *p* values shown in *parentheses* are from the post hoc test. *C*, representative retinal morphology in *rd3/rd3* (*top panel*) and *rd3/rd3 RD3GFP*$^{+}$ (*bottom panel*) littermates after 4 months of age. The photoreceptor layer is marked in *yellow*. *D*, linear density of photoreceptor nuclei per 100 μm of the retina section in WT (*filled circles*), *rd3/rd3* (*open circles*), *rd3/rd3 RD3GFP*$^{+}$ (*filled triangles*), and *rd3/*^{wt}*RD3GFP*$^{+}$ (*open triangles*) mice. The differences were evaluated by ANOVA ($F = 139$; $p < 0.0001$) and Bonferroni post hoc pairs comparison (99% CI, $\alpha = 0.01$). The *p* values shown in the graph are from the post hoc test. *RPE*, retinal pigment epithelium; *ONL*, outer nuclear layer; *OPL*, outer plexiform layer; *INL*, inner nuclear layer; *IPL*, inner plexiform layer; *GCL*, ganglion cell layer.

expressing transgene into a *GCAPs*$^{-/-}$ background (Fig. 6), the RD3GFP fluorescence was no longer restricted to the rod inner segment—it even became preferentially concentrated in rod outer segments.

Discussion

Biological function of RD3 in photoreceptors

Two possible roles were proposed and supported by experimental evidence for the RD3 in regulation of photoreceptor guanylyl cyclase—to promote cyclase accumulation in photoreceptors (18–20) and to inhibit the cyclase activity prior to its reaching the outer segment (21, 22). Evidently, the role of RD3 in maintaining the RetGC levels is most critical for the function of photoreceptors—the phototransduction becomes inefficient when the cGMP synthesis is impaired, forcing most of the cGMP gated channels that would be normally open in the dark to become closed (17, 22, 26) (Fig. 1*B*). However, when it comes to the role of RD3 in protecting photoreceptors from degeneration, our data indicate that the inhibitory capacity of RD3 is most essential for their survival, even more essential than maintaining the RetGC levels in the outer segment. Indeed, we previously observed (22) that photoreceptors in RetGC1$^{-/-}$ RetGC2$^{-/-}$ double knockout, completely devoid of the photoreceptor cyclase activity (27, 28), degenerate much slower than *rd3/rd3* photoreceptors, who retain low yet clearly detectable levels of RetGC, but are unable to suppress that residual cyclase activity by RD3. Our present study agrees with the hypothesis that the prevention of premature/aberrant RetGC activation by GCAPs, most likely in the inner segment, is crucial for the photoreceptor survival (Fig. 7). Although the levels of the cyclase activity in *rd3/rd3* mice are strongly suppressed because of the compromised delivery and/or accumulation of the enzyme in the outer segment, this does not explain the fast rate and the severity of the *rd3* photoreceptor degeneration. RetGC activity in *rd3/rd3GCAPs*$^{-/-}$ is not only reduced to the same low levels as in *rd3/rd3* but can no longer even become accelerated by GCAPs (Fig. 1). However, the lack of GCAPs drastically rescues the *rd3/rd3* photoreceptors (Fig. 2), evidently because even though there is still no RD3 to suppress the residual RetGC activity in these photoreceptors, there are also no GCAPs now to cause its aberrant activation—hence, the fast degeneration is averted (Fig. 7). Whereas the fast degeneration results from

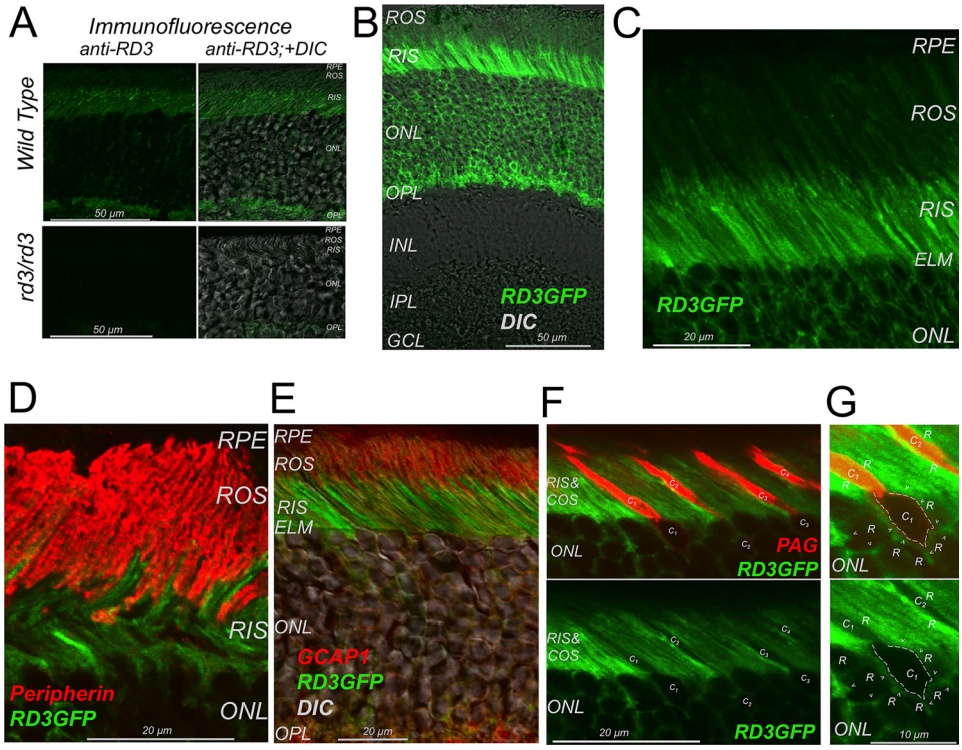

Figure 5. RD3 localization in mouse retina. *A*, immunofluorescence of the WT (*top panels*) and rd3/rd3 retinas (*bottom panels*) probed with anti-mouse RD3 polyclonal antibody; in each case, the fluorescence (*left panels*) was superimposed on DIC image (*right panels*). *B*, RD3GFP fluorescence in the retina of *RD3GFP*$^{+}$ transgenic mouse bread into C57B6J background. *C*, RD3GFP fluorescence in *rd3/rd3 RD3GFP*$^{+}$ retina, 9-μm Z-stack. *D*, RD3GFP fluorescence in *rd3/rd3 RD3GFP*$^{+}$ retina (*green*) superimposed on anti-peripherin immunofluorescence (*red*). *E*, RD3GFP fluorescence in *rd3/rd3 RD3GFP*$^{+}$ retina (*green*) superimposed on anti-GCAP1 immunofluorescence (*red*) and DIC image. *F* and *G*, testing for RD3GFP expression in *rd3/rd3RD3GFP*$^{+}$ cones. *Upper panels*, RD3GFP fluorescence (*green*) superimposed on cone-specific rhodamine-conjugated peanut agglutinin fluorescence (*PA*, *red*). *Lower panels*, RD3GFP fluorescence alone. *F*, four PA-positive cones in the frame are marked C_1 through C_4. Note that the C_1–C_4 cones in the *lower panel* appear as dark contours surrounded by the fluorescent rod inners segments. *G*, fragment of the C_1 cone cell from *F* shown at higher magnification and after a stronger γ adjustment applied to the whole panel. The *dashed line* marks the peanut agglutinin–positive (*top panel*) surface of the cone cell body. *Arrowheads* indicate the RD3GFP fluorescence in the cytoplasm of the surrounding rod cell bodies (*R*). In the *bottom panel*, note the absence of detectable RD3GFP fluorescence in the cone cell body. *RPE*, retinal pigment epithelium; *ROS*, rod outer segments; *ONL*, outer nuclear layer; *OPL*, outer plexiform layer; *INL*, inner nuclear layer; *IPL*, inner plexiform layer; *GCL*, ganglion cell layer; *RIS*, rod inner segments; *COS*, cone outer segments; *ELM*, external limiting membrane; *PAG*, peanut agglutinin.

GCAP-mediated cyclase activation in the absence of RD3, the remaining—much slower—loss of photoreceptors in *rd3/rd3GCAPs*$^{-/-}$ could result from constitutively low activity cGMP gated channels in the outer segment triggering slow degeneration (22, 28, 29). However, it could also be a result of incomplete inhibition of the cyclase by RD3. RD3 normally inhibits both GCAP-stimulated and the basal activity of the cyclase (21, 22). Because the basal activity of RetGC is detectable in *rd3/rd3* (Fig. 1*A*) and remains detectable even in *rd3/rd3GCAPs*$^{-/-}$, it is conceivable that not only GCAP-stimulated activity, but, to a lesser extent, the basal activity of the cyclase remaining in *rd3/rd3GCAPs*$^{-/-}$ when unrestrained by RD3 is sufficient to eventually cause the degeneration.

The processes triggered downstream from deregulation of the cyclase in the absence of RD3 are yet to be delineated in the future studies, but regardless of what these processes could be, they are most likely triggered in the inner segment (Fig. 7). The localization of RD3, both of the endogenous protein in WT and of the GFP-tagged transgenic product, argue that RD3 predominantly operates in the inner segment (Figs. 4–6). The lack of RD3 immunofluorescence in the outer segment that we observed (Fig. 4*A*) is very unlikely to be a result of a simple epitope masking, because Zulliger *et al.* (20) reported a similar result using independently produced antibody. Furthermore, the intrinsic fluorescence of RD3GFP demonstrates pattern of distribution between the inner and outer segments similar to the endogenous RD3 immunofluorescence (Fig. 5). Because the transgenically expressed RD3GFP effectively substitutes for the endogenous RD3 in *rd3/rd3* photoreceptors (Figs. 3 and 4), this compartmentalization of RD3GFP must reflect the normal distribution of a functional RD3 rather than accumulation in the inner segment of a misfolded inactive protein.

The disparity in RD3 distribution between the two cellular compartments documented in our study and in Ref. 20 appears to be at odds with a report (23) stating that RD3 accumulates in both outer and inner segment, as well as in any other layer of the retina. In that report, however, the specificity of the antibody was not tested using *rd3/rd3* retinas as a negative control, and therefore the results of the immunofluorescence in Ref. 23 could be affected by nonspecific cross-reactivity of the primary antibody.

It is also important that the absence of GCAPs strongly alters the RD3GFP fluorescence distribution between the inner and outer segment (Fig. 6), consistent with the earlier observation by Zulliger *et al.* (20) that the RD3 levels in GCAPs$^{-/-}$ ROS become elevated. Our results favor the hypothesis of the competition between RD3 and GCAPs for the cyclase in different cellular compartments (21, 22) (Fig. 7). Based on the kinetic

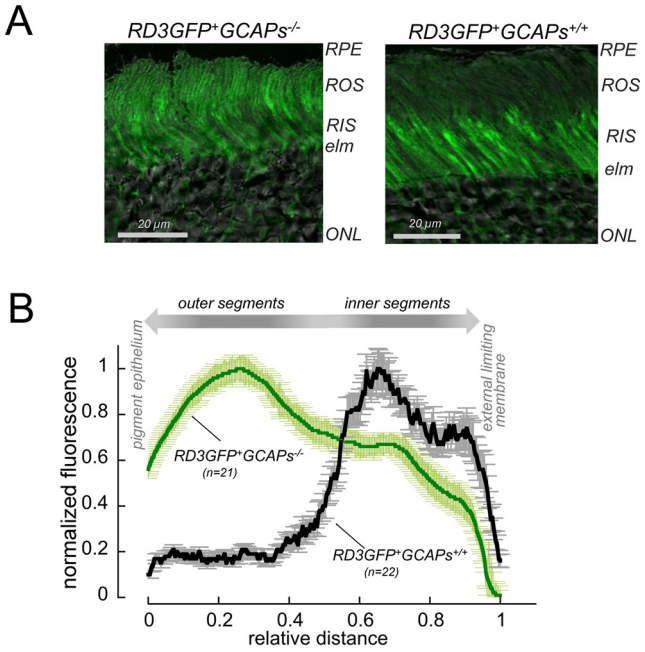

Figure 6. Elimination of GCAPs promotes migration of RD3GFP to the outer segment. *A*, RD3GFP fluorescence in retinal sections from mice lacking GCAPs (*RD3GFP*$^{+}$*GCAPs*$^{-/-}$, *left panel*) *versus RD3GFP*$^{+}$*GCAPs*$^{+/+}$ (*right panel*) retinas; superimposed on DIC. *B*, average distribution of the RD3GFP fluorescence (normalized by maximal fluorescence intensity in each case) across the posterior portion of rod layer, relative to the distance from retinal pigment epithelium to the external limiting membrane in each case, in *RD3GFP*$^{+}$*GCAPs*$^{+/+}$ (*black trace*, mean average; *gray*, S.E.; *error bars*, $n = 22$) and *RD3GFP*$^{+}$*GCAPs*$^{-/-}$ (*dark green trace*, mean average; *light-green*, S.E.; *error bars*, $n = 21$). Outer segments are predominant in the stratum proximal to RPE, and the inner segments are predominant in the stratum proximal to the external limiting membrane. *RPE*, retinal pigment epithelium; *ROS*, rod outer segments; *ONL*, outer nuclear layer; *RIS*, rod inner segments; *elm*, external limiting membrane.

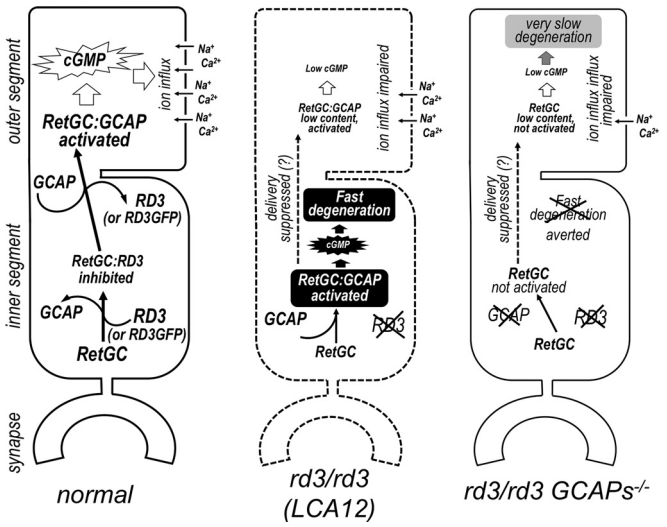

Figure 7. Biological role of RD3 in maintaining viability of photoreceptor cells. *Left panel*, the schematics of a normal function of RD3 in photoreceptors. RD3 regulation of the cyclase is dual: to help accumulate RetGC in the outer segment and to block RetGC activity in the inner segment. The endogenous RD3 (as well as RD3GFP in transgenic mice) prevents activation of RetGC by GCAPs while the cyclase is in transit to the outer segment, at the end of which GCAPs displace RD3 from the complex with the cyclase and put RetGC under control of the negative calcium feedback to accelerate re-opening of cGMP gated channels after photoexcitation. *Middle panel*, in *rd3/rd3* mouse photoreceptors as well as those in LCA12 patients, the content of RetGC in the outer segment is reduced, but the fast degeneration in this case results not from the low content of the cyclase but from the lack of the ability to block aberrant activation of RetGC by GCAPs in the inner segment. *Right panel*, elimination of GCAPs further aggravates the deficiency of cGMP production in *rd3/rd3* photoreceptors but averts the fast degeneration, because even in the absence of RD3 the cyclase now does not become activated in the inner segment. See "Discussion" for other details.

studies (21, 22), RD3 and GCAP reduce each other's apparent affinities for the cyclase. Evidently, the inhibitory action of RD3 prevents GCAPs from binding to the cyclase while in the inner segment. This trend must become reversed as the cyclase enters the outer segment, where GCAPs now replace RD3 and put the cyclase under control of the negative calcium feedback. Competition with GCAPs would normally restrict RD3 from accumulating in the outer segment, but in GCAPs$^{-/-}$ photoreceptors, where RD3 faces no such competition, it has a better chance of reaching the outer segment in the complex with the guanylyl cyclase.

Currently little is known about the mechanisms of RD3 interaction with the cyclase. The structures of GCAPs (30–32) and recently RD3 (33) have been established; however, the structure of the cyclase itself still presents a major barrier for understanding the molecular dynamics of the complex. To date, the three-dimensional structure of RetGC has been resolved only for its catalytic core (34, 35), not for those domains that present most important regulatory parts. The regulatory binding of GCAP1 and GCAP2 to the cyclase most critically involves the kinase homology and dimerization domains of RetGC (36, 37), but in case of RD3 its interaction with the cyclase appears somewhat more complex. The mutational analyses indicate that, in contrast to GCAPs (36, 37), a portion proximal to the C terminus of RetGC is critical for RD3 binding (19). However, in addition to that, some point mutations in the kinase homology domain (but not dimerization domain) of the cyclase also disable the RD3 binding (36, 37). RD3 and GCAP (11, 17) not only have highly dissimilar protein sequences (<5% overall identity and <9% similarity in pairwise alignment; European Bioinformatics Institute EMBOS Needle on-line tool) but also drastically dissimilar three-dimensional structures. The guanylyl cyclase-binding interface on RD3 (22, 33) occupies the central part of RD3 elongated bundle of α-helices, whereas the cyclase-binding interface of GCAP occupies portions of three helix–loop–helix EF-hand domains (38). This suggests that most likely the binding sites for RD3 and GCAP on RetGC are also nonidentical. The opposite effects of GCAPs and RD3 (21, 22) (Fig. 3) on the cyclase activity, however, could indicate that the binding interfaces for GCAPs and RD3 on RetGC are partially overlapped or are in a close proximity to each other in a three-dimensional structure of the cyclase. Nonetheless, the mutually restrictive binding of RD3 and GCAP does not exclude a possibility of a loner-distance allosteric interference via nonoverlapping interfaces, such that binding of one regulatory protein causes, through a rearrangement of the quaternary structure of the cyclase dimer, hindrance for the binding of the other regulatory protein. The structure of the RD3–RetGC complex, the mechanisms of GCAP displacement by RD3 and vice versa, together with the pathways of the photoreceptor degeneration triggered by RetGC in the inner segment, remain the major questions for the future studies.

Experimental procedures

Animals

All experiments involving animals were conducted in accordance with the Public Health Service guidelines and approved by the Salus University Institutional Animal Care and Use Committee. The WT C57B6J and *rd3*/*rd3* mouse strains were purchased from JAX Research/Jackson's Laboratory. Mice of other genotypes used in this study were kindly provided by other investigators: *RetGC1*$^{-/-}$ line GCE null (27) by Dr. David Garbers (University of Texas), *RetGC2*$^{-/-}$ (28) by Dr. Wolfgang Baehr (University of Utah), and *GCAPs*$^{-/-}$ (13) by Dr. Jeannie Chen (University of Southern California). All mouse lines were made congenic to the C57B6 background by repetitive breeding for over 10 generations prior to conducting the experiments (22).

RD3 expression and purification

A human RD3GFP cDNA was constructed using the "splicing by overlap extension" method (39) as previously described in full detail (22). Recombinant human RD3, either untagged or tagged with eGFP (Clontech), was expressed from a pET11d vector in a BL21(DE3) Codon Plus *E. coli* strain (Stratagene/Agilent Technologies) induced by isopropyl-β-D-thiogalactopyranoside, extracted from the inclusion bodies, and purified by salt precipitation and dialysis as previously described (21, 22).

RD3GFP transgenic mice

The expression construct was assembled in a Stratagene pBluescript plasmid as follows. The human RD3GFP cDNA was PCR-amplified from a pQBI-fN3 construct previously used for RD3GFP expression in HEK293 cells (37) by PhusionFlash DNA polymerase (Thermo Fisher) using 5′-GGGAGAAAACTCGAGGGGCCAGGGGCTATGTCTCTCATCT and 5′-ATAGAGGATCCTCAGTCGGCTTTGGGCGCCCGGAAT primers and inserted into the XhoI/BamHI sites of a plasmid harboring 4.2-kb 5′-UTR of a mouse rod opsin gene (KpnI/XhoI fragment) and a modified polyadenylation signal fragment of the last exon of a mouse protamine *Mp1* gene (24) inserted in the BamHI/XbaI sites of pBluescript. The construct was verified using automated Sanger sequencing on both strands. The 6.3-kb fragment containing the transgenic construct excised by the PvuI/XbaI and purified from agarose gel was injected in male pronuclei of fertilized mouse eggs (service of the University of Michigan Transgenic Animal Model Core). The tail DNA samples from the F_0 founders and later of their progeny were tested for the presence of the RD3GFP transgene by PCR using a pair of primers, 5′-GGTCCACCTATGACCTCAGCCCCAT (f1) and 5′-TGACAGAGAACTTGTGGCCGTTAACAT (r1), generating 0.5-kb RD3GFP-specific fragment (Fig. 3*C*). The transgene-positive line was then maintained by crossing to the C57B6J and to rd3/rd3 mice in the C57B6J background (22).

Mouse Rd3 gene genotyping

A 0.6-kb fragment of the gene containing part of the *Rd3* exon 3 and the adjacent portion of intron 2 was PCR-amplified from tail DNA samples using high-fidelity Phusion Flash DNA polymerase (Thermo Scientific) and a pair of primers, 5′-CCTCAGAACTTTGTCCCTGTCAGCCA and 5′-GGTGATTGCCCTGGGTGGTCAGT, purified using a Zymo Research DNA cleanup kit, and subjected to automated Sanger sequencing using a primer, 5′-ATGTCACTGGCAAAGGGTGCGAT, to identify the WT, heterozygous *rd3*, and homozygous *rd3*/*rd3* by the presence of a stop codon-generating C → T transition (17).

GCAP1 expression and purification

Myristoylated bovine GCAP1 for *in vitro* assays was expressed from pET11d vector in a BLR(DE3) *E. coli* strain (both from Novagen/Calbiochem) harboring a pBB131 plasmid coding for a yeast *N*-myristoyl transferase and purified by calcium precipitation, butyl-Sepharose, and Sephacryl S-100 chromatography using a previously published procedure (40, 41). The purity of GCAP1 preparations estimated by SDS gel electrophoresis was ≥90%.

RetGC1 expression and guanyly cyclase activity assays

Human recombinant RetGC1 was expressed from a modified Invitrogen pRCCMV vector in HEK293 cells transfected using calcium-phosphate precipitation method, and the membrane fraction containing the expressed cyclase was purified as previously described (42). The guanylyl cyclase activity was assayed as previously described in detail in Ref. 42 with modification described in Ref. 22. In brief, the assay mixture (25 μl) containing HEK293 membranes, 30 mM MOPS-KOH (pH 7.2), 60 mM KCl, 4 mM NaCl, 1 mM DTT, 2 mM Ca^{2+}/Mg^{2+}/EGTA buffers, 0.9 mM free Mg^{2+}, 0.3 mM ATP, 4 mM cGMP, 1 mM GTP, 1 μCi of [α-^{32}P]GTP, 100 μM zaprinast and dipyridamole, and 10 mM creatine phosphate/0.5 unit of creatine phosphokinase (Sigma–Aldrich) was incubated at 30 °C for 30 min, and the reaction was stopped by heat inactivation at 95 °C for 2 min. The resultant [^{32}P]cGMP product was separated by TLC using fluorescently backed polyethyleneimine cellulose plates (Merck) developed in 0.2 M LiCl, cut from the plate, and eluted with 2 M LiCl in scintillation vials, and the radioactivity was counted using liquid scintillation. Mouse retinas for RetGC activity measurements were excised from the dark-adapted ~3.5-week-old mice using IR illumination (Kodak number 11 IR filters) and a dissecting microscope fitted with an Excalibur IR goggles as described, wrapped in aluminum foil, frozen in liquid N_2, and stored at −70 °C prior to their use in the cyclase activity assays conducted under IR illumination. The incubation time for the reaction was 12 min. The assay contained [^{3}H]cGMP internal standard to ensure the lack of cGMP product hydrolysis by light-activated phosphodiesterase. Ca^{2+}/EGTA buffers at 0.9 mM physiological for the photoreceptors (43) free Mg^{2+} were prepared using Tsien and Pozzan method (44) and verified by fluorescent indicator dyes as previously described in detail (40). Data fitting was performed using Synergy Kaleidagraph 4 software.

Electroretinography

The mice were dark-adapted overnight, their pupils were dilated by applying 1% tropicamide and 2.5% phenylephrine ophthalmic eye drops under dim red safelight illumination, and

then the mice were dark-adapted for another 10 min. Full-field ERG in mice anesthetized by inhalation of 1.7–1.9% isoflurane (VEDCO) was performed in the dark as previously described in detail (46, 47) using a Phoenix Research Laboratories Ganzfeld ERG2 setup. Series of 505-nm 0.1–1-ms light pulses (up to 1.1×10^6 photoisomerizations/rod) were delivered through IR camera-guided corneal electrode/LED light source, and 3–10 traces for each flash strength in series were averaged. Constant 505-nm illumination ($\sim 33 \times 10^3$ photoisomerizations/rod/s) was used as a background light to record photopic (cone) ERG responses to 1-ms 505-nm equivalent of 5.4×10^5 photoisomerizations/rod and delivered at 1-s intervals; traces were typically averaged from 10 to 15 trials for each animal.

Retinal morphology

The mice were anesthetized with a lethal dose of ketamine/xylazine injection and perfused through the heart with PBS and then with 2.5% glutaraldehyde in PBS. The eyes were surgically removed and fixed overnight in 2.5% glutaraldehyde, 2.5% formaldehyde, PBS solution (Electron Microscopy Sciences) at 4 °C. The fixed eyes were washed in PBS, soaked in PBS overnight, processed for paraffin embedding, sectioned, and stained with hematoxylin/eosin (AML Laboratories, St. Augustine, FL). The retinas were photographed using an Olympus Magnafire camera mounted on an Olympus BX21 microscope. The photoreceptor nuclei in the outer nuclear layer of the retina were counted from the 425-μm fragment of the 5-μm-thick retina section between the optic nerve and the periphery, and the density of the nuclei per 100 μm was averaged for each genotype.

Antibodies and immunoblotting

Rabbit RD3 polyclonal antibody 10929 was produced against purified recombinant mouse RD3 expressed in *E. coli* as described in Refs. 21, 22; GCAP1 and RetGC1 rabbit polyclonal antibodies were characterized previously (45, 48), rabbit polyclonal anti-peripherin antibody was a gift from Dr. Andrew Goldberg (Oakland University), and rabbit polyclonal anti-GAPDH antibody was purchased from an Invitrogen/Thermo Fisher Scientific (catalog no. PA1987).

Retinas from 3.5-week-old mice were excised in 20 μl of 10 mM Tris-HCl, pH 7.4, containing 1:100 dilution of protease inhibitor mixture concentrate (Millipore–Sigma) and homogenized in a radioimmune precipitation assay mixture of detergents for protein extraction (Abcam) containing the protease inhibitors, 300 μl/6 retinas. After 1 h of extraction on ice, the insoluble material was removed by centrifugation at 14,000 $\times$ *g*, 4 °C, and the protein extract was mixed with equal volumes of 2× Laemmli SDS sample buffer (Millipore–Sigma) and subjected to electrophoresis in 15% or 7% polyacrylamide gel containing 0.1% SDS. Following the electrophoresis, the proteins were transferred overnight at 50 V to polyvinylidene difluoride Immobilon P membrane (Millipore) at 18 °C using Tris–glycine transfer buffer (Novex/Invitrogen). The membranes were transiently stained by Ponceau S (Sigma) dye solution in 1% acetic acid to mark the positions of molecular mass markers, destained by series of washes in water and TBS (Fisher Scientific) containing 0.5% Tween 20 (TTBS), and blocked by Super Block (ThermoFisher) solution in TTBS, probed by primary antibody, and the luminescence was developed using peroxidase-conjugated goat anti-rabbit polyclonal IgG (Cappel/MP Biomedical) and a Pierce Super-Signal Femto substrate protocol (Thermo Scientific). The images were acquired using a Fotodyne Luminous FX imager and subjected to densitometry using ImageJ software (National Institutes of Health).

Confocal microscopy

The mice were perfused with the fixative solution as described above except that 10% freshly prepared formaldehyde solution in PBS was used instead of glutaraldehyde. The eyes were then dissected, and the eyecups were placed into 10% formaldehyde/PBS for 5 min and then 5% formaldehyde/PBS for 12 h at 4 °C. The fixed eyecups were washed in PBS, impregnated with 30% sucrose in PBS, and frozen at −70 °C in OCT medium (Electron Microscopy Sciences). The cryosections were taken using a Hacker–Bright cryogenic microtome, dried for 1 h at room temperature, and stored in −70 °C. The sections were washed three times in PBS containing 0.1 M glycine (pH 7.4), blocked for 1 h at 30 °C with the same solution containing 5% BSA and 0.1% Triton X-100, incubated overnight at 4 °C, incubated for 1 h at room temperature with the primary antibody, then washed with PBS solution three times for 15 min each, incubated with the 1:400 diluted donkey anti-rabbit Alexa Fluor 568 – or Alexa Fluor 488 – conjugated antibody (Molecular Probes/Thermo Fisher), and washed four times with PBS for 15 min each at room temperature. Where indicated, the cones were labeled by incubating retinal sections with rhodamine-conjugated peanut agglutinin (Vector Laboratories), 5 μg/ml, overnight at 4 °C, and washed three times with PBS for 15 min each at room temperature. The sections were covered with Vectashield mounting medium (Vector Laboratories), and confocal images were acquired using an Olympus FV1000 spectral instrument controlled by FluoView FV10-ASW software, collecting in a sequential mode images excited by 488- and 543-nm lasers. Fluorescence of RD3GFP was recorded using excitation at 488 nm. Where indicated, fluorescence was superimposed on a differential interference contrast (DIC) image. No changes were made to the original images except for γ correction applied to the whole image for clarity of presentation in the print. Fluorescence distribution, where indicated, was quantified using unmodified images.

Statistics

Statistical significance of the differences was tested by ANOVA/Bonferroni post hoc multiple-pairs comparison test (confidence interval 99%; $\alpha = 0.01$) using Synergy Kaleidagraph 4 software.

Author contributions—A. M. D. conceptualization; A. M. D., E. V. O., and I. V. P. data curation; A. M. D. supervision; A. M. D. funding acquisition; A. M. D. and I. V. P. investigation; A. M. D., E. V. O., and I. V. P. methodology; A. M. D. writing-original draft; I. V. P. formal analysis.

Acknowledgment—We thank Dr. Andrew Goldberg for the generous gift of anti-peripherin antibody.

References

1. Dizhoor, A. M., Lowe, D. G., Olshevskaya, E. V., Laura, R. P., and Hurley, J. B. (1994) The human photoreceptor membrane guanylyl cyclase, RetGC, is present in outer segments and is regulated by calcium and a soluble activator. *Neuron* **12,** 1345–1352 CrossRef Medline
2. Lowe, D. G., Dizhoor, A. M., Liu, K., Gu, Q., Spencer, M., Laura, R., Lu, L., and Hurley, J. B. (1995) Cloning and expression of a second photoreceptor-specific membrane retina guanylyl cyclase (RetGC), RetGC-2. *Proc. Natl. Acad. Sci. U.S.A.* **92,** 5535–5539 CrossRef Medline
3. Yang, R. B., Foster, D. C., Garbers, D. L., and Fülle, H. J. (1995) Two membrane forms of guanylyl cyclase found in the eye. *Proc. Natl. Acad. Sci. U.S.A.* **92,** 602–606 CrossRef Medline
4. Arshavsky, V. Y., Lamb, T. D., and Pugh, E. N., Jr. (2002) G proteins and phototransduction. *Annu. Rev. Physiol.* **64,** 153–187 CrossRef Medline
5. Dizhoor, A. M., Olshevskaya, E. V., and Peshenko, I. V. (2010) Mg^{2+}/Ca^{2+} cation binding cycle of guanylyl cyclase activating proteins (GCAPs): role in regulation of photoreceptor guanylyl cyclase. *Mol. Cell. Biochem.* **334,** 117–124 CrossRef Medline
6. Koch, K.-W., and Dell'Orco, D. (2015) Protein and signaling networks in vertebrate photoreceptor cells. *Front. Mol. Neurosci.* **8,** 67 Medline
7. Fu, Y., and Yau, K.-W. (2007) Phototransduction in mouse rods and cones. *Pflugers Arch.* **454,** 805–819 CrossRef Medline
8. Pugh, E. N., Jr., Nikonov, S., and Lamb, T. D. (1999) Molecular mechanisms of vertebrate photoreceptor light adaptation. *Curr. Opin. Neurobiol.* **9,** 410–418 CrossRef Medline
9. Palczewski, K., Subbaraya, I., Gorczyca, W. A., Helekar, B. S., Ruiz, C. C., Ohguro, H., Huang, J., Zhao, X., Crabb, J. W., and Johnson, R. S. (1994) Molecular cloning and characterization of retinal photoreceptor guanylyl cyclase-activating protein. *Neuron* **13,** 395–404 CrossRef Medline
10. Dizhoor, A. M., Olshevskaya, E. V., Henzel, W. J., Wong, S. C., Stults, J. T., Ankoudinova, I., and Hurley, J. B. (1995) Cloning, sequencing, and expression of a 24-kDa Ca^{2+}-binding protein activating photoreceptor guanylyl cyclase. *J. Biol. Chem.* **270,** 25200–25206 CrossRef Medline
11. Imanishi, Y., Yang, L., Sokal, I., Filipek, S., Palczewski, K., and Baehr, W. (2004) Diversity of guanylate cyclase-activating proteins (GCAPs) in teleost fish, characterization of three novel GCAPs (GCAP4, GCAP5, GCAP7) from zebrafish (*Danio rerio*) and prediction of eight GCAPs (GCAP1–8) in pufferfish (*Fugu rubripes*). *J. Mol. Evol.* **59,** 204–217 CrossRef Medline
12. Koch, K. W., and Stryer, L. (1988) Highly cooperative feedback control of retinal rod guanylate cyclase by calcium ions. *Nature* **334,** 64–66 CrossRef Medline
13. Mendez, A., Burns, M. E., Sokal, I., Dizhoor, A. M., Baehr, W., Palczewski, K., Baylor, D. A., Chen, J. (2001) Role of guanylate cyclase-activating proteins (GCAPs) in setting the flash sensitivity of rod photoreceptors. *Proc. Natl. Acad. Sci. U.S.A.* **98,** 9948–9953 CrossRef Medline
14. Burns, M. E., Mendez, A., Chen, J., Baylor, D. A. (2002) Dynamics of cyclic GMP synthesis in retinal rods. *Neuron* **36,** 81–91 CrossRef Medline
15. Sakurai, K., Chen, J., and Kefalov, V. J. (2011) Role of guanylyl cyclase modulation in mouse cone phototransduction. *J. Neurosci.* **31,** 7991–8000 CrossRef Medline
16. Makino, C. L., Wen, X. H., Olshevskaya, E. V., Peshenko, I. V., Savchenko, A. B., and Dizhoor, A. M. (2012) Enzymatic relay mechanism stimulates cyclic GMP synthesis in rod photoresponse, biochemical and physiological study in guanylyl cyclase activating protein 1 knockout mice. *PLoS One* **7,** e47637 CrossRef Medline
17. Friedman, J. S., Chang, B., Kannabiran, C., Chakarova, C., Singh, H. P., Jalali, S., Hawes, N. L., Branham, K., Othman, M., Filippova, E., Thompson, D. A., Webster, A. R., Andréasson, S., Jacobson, S. G., Bhattacharya, S. S., *et al.* (2006) Premature truncation of a novel protein, RD3, exhibiting subnuclear localization is associated with retinal degeneration. *Am. J. Hum. Genet.* **79,** 1059–1070 CrossRef Medline
18. Molday, L. L., Jefferies, T., and Molday, R. S. (2014) Insights into the role of RD3 in guanylate cyclase trafficking, photoreceptor degeneration, and Leber congenital amaurosis. *Front. Mol. Neurosci.* **7,** 44 Medline
19. Azadi, S., Molday, L. L., and Molday, R. S. (2010) RD3, the protein associated with Leber congenital amaurosis type 12, is required for guanylate cyclase trafficking in photoreceptor cells. *Proc. Natl. Acad. Sci. U.S.A.* **107,** 21158–21163 CrossRef Medline
20. Zulliger, R., Naash, M. I., Rajala, R. V., Molday, R. S., and Azadi, S. (2015) Impaired association of retinal degeneration-3 with guanylate cyclase-1 and guanylate cyclase-activating protein-1 leads to Leber congenital amaurosis-1. *J. Biol. Chem.* **290,** 3488–3499 CrossRef Medline
21. Peshenko, I. V., Olshevskaya, E. V., Azadi, S., Molday, L. L., Molday, R. S., and Dizhoor, A. M. (2011) Retinal degeneration 3 (RD3) protein inhibits catalytic activity of retinal membrane guanylyl cyclase (RetGC) and its stimulation by activating proteins. *Biochemistry* **50,** 9511–9519 CrossRef Medline
22. Peshenko, I. V., Olshevskaya, E. V., and Dizhoor, A. M. (2016) Functional study and mapping sites for interaction with the target enzyme in retinal degeneration 3 (RD3) protein. *J. Biol. Chem.* **291,** 19713–19723 CrossRef Medline
23. Wimberg, H., Janssen-Bienhold, U., and Koch, K.-W. (2018) Control of the nucleotide cycle in photoreceptor cell extracts by retinal degeneration protein 3 front. *Front. Mol. Neurosci.* **11,** 52 CrossRef Medline
24. Raport, C. J., Lem, J., Makino, C., Chen, C. K., Fitch, C. L., Hobson, A., Baylor, D., Simon, M. I., and Hurley, J. B. (1994) Downregulation of cGMP phosphodiesterase induced by expression of GTPase-deficient cone transducin in mouse rod photoreceptors. *Invest. Ophthalmol. Vis. Sci.* **35,** 2932–2947 Medline
25. Jeon, C. J., Strettoi, E., and Masland, R. H. (1998) The major cell populations of the mouse retina. *J. Neurosci.* **18,** 8936–8946 CrossRef Medline
26. Molday, L. L., Djajadi, H., Yan, P., Szczygiel, L., Boye, S. L., Chiodo, V. A., Gregory-Evans, K., Sarunic, M. V., Hauswirth, W. W., and Molday, R. S. (2013) RD3 gene delivery restores guanylate cyclase localization and rescues photoreceptors in the Rd3 mouse model of Leber congenital amaurosis 12. *Hum. Mol. Genet.* **22,** 3894–3905 CrossRef Medline
27. Yang, R. B., Robinson, S. W., Xiong, W. H., Yau, K. W., Birch, D. G., and Garbers, D. L. (1999) Disruption of a retinal guanylyl cyclase gene leads to cone-specific dystrophy and paradoxical rod behavior. *J. Neurosci.* **19,** 5889–5897 CrossRef Medline
28. Baehr, W., Karan, S., Maeda, T., Luo, D. G., Li, S., Bronson, J. D., Watt, C. B., Yau, K. W., Frederick, J. M., and Palczewski, K. (2007) The function of guanylate cyclase 1 and guanylate cyclase 2 in rod and cone photoreceptors. *J. Biol. Chem.* **282,** 8837–8847 CrossRef Medline
29. Woodruff, M. L., Wang, Z., Chung, H. Y., Redmond, T. M., Fain, G. L., and Lem, J. (2003) Spontaneous activity of opsin apoprotein is a cause of Leber congenital amaurosis. *Nat. Genet.* **35,** 158–164 CrossRef Medline
30. Ames, J. B., Dizhoor, A. M., Ikura, M., Palczewski, K., and Stryer, L. (1999) Three-dimensional structure of guanylyl cyclase activating protein-2, a calcium-sensitive modulator of photoreceptor guanylyl cyclases. *J. Biol. Chem.* **274,** 19329–19337 CrossRef Medline
31. Stephen, R., Bereta, G., Golczak, M., Palczewski, K., and Sousa, M. C. (2007) Stabilizing function for myristoyl group revealed by the crystal structure of a neuronal calcium sensor, guanylate cyclase-activating protein 1. *Structure* **15,** 1392–1402 CrossRef Medline
32. Stephen, R., Palczewski, K., and Sousa, M. C. (2006) The crystal structure of GCAP3 suggests molecular mechanism of GCAP-linked cone dystrophies. *J. Mol. Biol.* **359,** 266–275 CrossRef Medline
33. Peshenko, I. V., Yu, Q., Lim, S., Cudia, D., Dizhoor, A. M., and Ames, J. B. (2019) Retinal degeneration 3 (RD3) protein, a retinal guanylyl cyclase regulator, forms a monomeric and elongated four-helix bundle. *J. Biol. Chem.* **294,** 2318–2328 CrossRef Medline
34. Liu, Y., Ruoho, A. E., Rao, V. D., and Hurley, J. H. (1997) Catalytic mechanism of the adenylyl and guanylyl cyclases: modeling and mutational analysis. *Proc. Natl. Acad. Sci. U.S.A.* **94,** 13414–13419 CrossRef Medline
35. Tucker, C. L., Hurley, J. H., Miller, T. R., and Hurley, J. B. (1998) Two amino acid substitutions convert a guanylyl cyclase, RetGC-1, into an

adenylyl cyclase. *Proc. Natl. Acad. Sci. U.S.A.* **95,** 5993–5997 CrossRef Medline

36. Peshenko, I. V., Olshevskaya, E. V., and Dizhoor, A. M. (2015) Evaluating the role of retinal membrane guanylyl cyclase 1 (RetGC1) domains in binding guanylyl cyclase-activating proteins (GCAPs). *J. Biol. Chem.* **290,** 6913–6924 CrossRef Medline
37. Peshenko, I. V., Olshevskaya, E. V., and Dizhoor, A. M. (2015) Dimerization domain of retinal membrane guanylyl cyclase 1 (RetGC1) is an essential part of guanylyl cyclase-activating protein (GCAP) binding interface. *J. Biol. Chem.* **290,** 19584–19596 CrossRef Medline
38. Peshenko, I. V., Olshevskaya, E. V., Lim, S., Ames, J. B., and Dizhoor, A. M. (2014) Identification of target binding site in photoreceptor guanylyl cyclase activating protein 1 (GCAP1). *J. Biol. Chem.* **289,** 10140–10154 CrossRef Medline
39. Horton, R. M., and Pease, L. R. (1991) Directed mutagenesis. In *Practical Approach* (McPherson, M. J., ed) pp. 217–250, Oxford University Press, Oxford, UK
40. Peshenko, I. V., and Dizhoor, A. M. (2006) Ca^{2+} and Mg^{2+} binding properties of GCAP-1: evidence that Mg^{2+}-bound form is the physiological activator of photoreceptor guanylyl cyclase. *J. Biol. Chem.* **281,** 23830–23841 CrossRef Medline
41. Peshenko, I. V., Cideciyan, A. V., Sumaroka, A., Olshevskaya, E. V., Scholten, A., Abbas, S., Koch, K.-W., Jacobson, S. G., and Dizhoor, A. M. (2019) A Gly86Arg mutation in the calcium-sensor protein GCAP1 alters regulation of retinal guanylyl cyclase and causes dominant cone-rod degeneration. *J. Biol. Chem.* **294,** 3476–3488 CrossRef Medline
42. Peshenko, I. V., Moiseyev, G. P., Olshevskaya, E. V., and Dizhoor, A. M. (2004) Factors that determine Ca^{2+} sensitivity of photoreceptor guanylyl cyclase: kinetic analysis of the interaction between the Ca^{2+}-bound and the Ca^{2+}-free guanylyl cyclase activating proteins (GCAPs) and recombinant photoreceptor guanylyl cyclase 1 (RetGC-1). *Biochemistry* **43,** 13796–13804 CrossRef Medline
43. Chen, C., Nakatani, K., and Koutalos, Y. (2003) Free magnesium concentration in salamander photoreceptor outer segments. *J. Physiol.* **553,** 125–135 CrossRef Medline
44. Tsien, R., and Pozzan, T. (1989) Measurement of cytosolic free Ca^{2+} with quin2. *Methods Enzymol.* **172,** 230–262 CrossRef Medline
45. Makino, C. L., Peshenko, I. V., Wen, X. H., Olshevskaya, E. V., Barrett, R., and Dizhoor, A. M. (2008) A role for GCAP2 in regulating the photoresponse: guanylyl cyclase activation and rod electrophysiology in GUCA1B knock-out mice. *J. Biol. Chem.* **283,** 29135–29143 CrossRef Medline
46. Dizhoor, A. M., Olshevskaya, E. V., and Peshenko, I. V. (2016) The R838S mutation in retinal guanylyl cyclase 1 (RetGC1) alters calcium sensitivity of cGMP synthesis in the retina and causes blindness in transgenic mice. *J. Biol. Chem.* **291,** 24504–24516 CrossRef Medline
47. Sato, S., Peshenko, I. V., Olshevskaya, E. V., Kefalov, V. J., and Dizhoor, A. M. (2018) GUCY2D cone-rod dystrophy-6 is a "phototransduction disease" triggered by abnormal calcium feedback on retinal membrane guanylyl cyclase 1. *J. Neurosci.* **38,** 2990–3000 CrossRef Medline
48. Laura, R. P., Dizhoor, A. M., Hurley, J. B. (1996) The membrane guanylyl cyclase, retinal guanylyl cyclase-1, is activated through its intracellular domain. *J. Biol. Chem.* **271,** 11646–11651 CrossRef Medline